Spatiotemporal dynamics of a unidirectional ring oscillator with photorefractive gain

G. D'Alessandro*
Department of Physics, University of Strathclyde, 107 Rottenrow, Glasgow G4 0NG, Scotland
(Received 31 December 1991; revised manuscript received 7 April 1992)

In a cavity with photorefractive gain the resonator field is fed by a pump beam through two-wave mixing inside a photorefractive crystal. In this paper we develop a simplified model for such a system which takes into account the transverse dependence of the pump and the resonator fields. We then study the onset of spatiotemporal structures both analytically and numerically.

PACS number(s): 42.65.−k

I. INTRODUCTION

In this paper we shall analyze an optical system like the one shown in Fig. 1: a pump beam E_P feeds energy to the resonator field E_R through two-wave mixing in a crystal of photorefractive material. Many experiments [1–5] have studied the dynamics of the resonator field in the transverse plane, i.e., in the plane orthogonal to the propagation direction. This system has a very rich spatiotemporal dynamics: the field can either reach a stationary state with varying degrees of spatial complexity or it can evolve in a periodic or even chaotic way [4, 5]. A model that takes into account only the longitudinal dependence of the field has been studied in Refs. [6, 7]. In this paper we obtain a set of equations that include the transverse coordinates' dependence of the electric field under suitable simplifying hypothesis: we shall assume that the slice of photorefractive material is very thin, so that the field structure in the transverse plane is mainly determined by diffraction in the cavity and by the pump width. The final equations are very similar to those of a homogeneously broadened unidirectional ring laser [8]; however in constrast to a typical laser model, one of the variables has a very slow dynamics, so that the model can be conveniently reduced.

In Sec. II we obtain a set of equations for the change of index of refraction in the photorefractive crystal; in Sec. III we apply the mean-field limit [8] to the resonator field; the two sets of equations are put together in Sec. IV. In Sec. V we discuss the linear stability analysis of the simplest stationary solutions; Sec. VI deals with numerical results. The conclusions are presented in Sec. VII.

II. EQUATIONS FOR THE PHOTOREFRACTIVE CRYSTAL

The aim of these first three sections is to obtain a very simple model for the dynamics of the resonator field in the transverse plane. To this end we shall make use of the mean-field-limit theory, developed in Refs. [8, 9]; we refer to those articles for a comprehensive description of it. Its main tenet is that the photorefractive medium is very short compared to the cavity length, so that the gain per single pass is very small. The dominant force that drives the dynamics in the transverse plane is thus diffraction during propagation through the cavity. The advantage of this approach is that the equation for the field inside the medium can be simplified greatly by using the hypothesis that the gain and the length of the material are small; the equation outside the photorefractive medium itself is just a free-space propagation equation and can be formally integrated in the direction of the cavity axis. The final result is an equation which does not contain any longitudinal dependence.

The pump and resonator fields are represented by two plane waves with slowly varying amplitudes. The pump field amplitude F_P is spatially varying but constant in time:

$$E_P(\mathbf{x},t) = F_P(\mathbf{x})e^{i(\mathbf{K}_P\cdot\mathbf{x}-\omega_P t)} + \text{c.c.},$$

where $\mathbf{K}_P$ and ω_P are, respectively, the pump wave vector and frequency. The resonator field amplitude F_R is time dependent:

$$E_R(\mathbf{x},t) = F_R(\mathbf{x},t)e^{i(\mathbf{K}_R\cdot\mathbf{x}-\omega_R t)} + \text{c.c.}$$

Here $\mathbf{K}_R$ and ω_R are, respectively, the wave vector of a reference resonator mode and the real frequency of oscillation of the resonator field (an unknown quantity at this stage). We shall always suppose that the resonator field is much less intense than the pump field $|F_P| \gg |F_R|$. The intensity of the total optical field in the photorefractive material

$$\mathcal{E}(\mathbf{x},t) = E_P(\mathbf{x},t) + E_R(\mathbf{x},t) \tag{1}$$

can then be written as

$$I(\mathbf{x},t) \equiv |\mathcal{E}(\mathbf{x},t)|^2 \simeq I_0(\mathbf{x})[1 + M(\mathbf{x},t)]. \tag{2}$$

$I_0(\mathbf{x}) \equiv |F_P|^2 + |F_R|^2 \simeq |F_P(\mathbf{x})|^2$ can be considered approximately constant in time. $M(\mathbf{x},t)$ is the modulation due to the interference between the two beams:

$$M(\mathbf{x},t) = \frac{F_P F_R^* e^{i(\mathbf{K}_{PR}\cdot\mathbf{x}-\delta_{PR}t)}}{|F_P|^2 + |F_R|^2} + \text{c.c.},$$

where

$$\mathbf{K}_{PR} = \mathbf{K}_P - \mathbf{K}_R, \quad \delta_{PR} = \omega_P - \omega_R. \tag{3}$$

Note that $\mathbf{K}_{PR}$ is zero only if the two beams are parallel and have exactly the same wavelength. In this case, there is no interaction between the pump and resonator beams; actually there is no resonator field. In more "normal" situations, when the pump beam makes an angle with the cavity axis, $\mathbf{K}_{PR}$ is of the same order of magnitude of the light wave vector. δ_{PR} instead is usually much smaller than the optical frequencies: we will see later (Sec. V) that the frequency of the resonator field is pulled very strongly toward the pump frequency so that δ_{PR} is a detuning of the order of a kilohertz.

We use a band transport model for the photorefractive material [10–13]. The valence band of the material is fully occupied, while the conduction band is empty. In the band gap there is a level of donor atoms and, slighty lower, a level of acceptor atoms. In the dark the acceptor atoms are fully ionized by the donor atoms, which usually are much more numerous. Suppose that we illuminate in a nonuniform way the crystal: in the bright regions the electrons are excited from the donor level to the conduction band where they can diffuse. Eventually they recombine with excited donors in the dark regions of the crystal. In this way the illuminated parts acquire a positive charge, while the dark areas are negatively charged. An electric field forms inside the material and changes its refractive index of the material through the electro-optic effect.

The equations that describe such a model are [12]

$$\frac{\partial N_D^+}{\partial t} = \left[\left(\frac{\alpha_D}{h\nu}\right) I(\mathbf{x},t) + \beta\right](N_D - N_D^+) - \gamma_D \tilde{n}_e N_D^+, \tag{4}$$

$$\frac{\partial \tilde{n}_e}{\partial t} - \frac{\partial N_D^+}{\partial t} = \frac{k_B T \mu}{e}\nabla^2 \tilde{n}_e + \frac{\mu e \tilde{n}_e}{\epsilon}(N_D^+ - \tilde{n}_e - N_A) - \mu \nabla \tilde{n}_e \cdot (\nabla \tilde{\varphi} - \mathbf{E}_A), \tag{5}$$

$$\nabla^2 \tilde{\varphi} = -\frac{e}{\epsilon}(N_D^+ - \tilde{n}_e - N_A). \tag{6}$$

Equation (4) is a rate equation, Eq. (5) is the continuity equation, and Eq. (6) is Poisson's law for the internal electric field. N_D is the total donor density, N_D^+ is the density of the excited donors, while $\tilde{n}_e$ is that of the electrons. N_A is the density of acceptor atoms, which are supposed to be fully occupied. $\tilde{\varphi}$ is the internal electric potential generated by the electrons and the excited donor atoms. α_D is the absorption cross section of the donor atoms, β is the thermal carrier generating rate, γ_D is the recombination coefficient of a free electron at an N_D^+ site, and $I(\mathbf{x},t)$ is the total light intensity illuminating the slice. μ is the electrons mobility, e is the absolute value of their charge, k_B is the Boltzmann constant, T is the absolute temperature, and ϵ is the dielectric constant of the material. Finally, $\mathbf{E}_A$ is an externally applied electric field.

The main steps that are needed to simplify these equations are as follows. (i) Neglect the thermal carrier generating rate β. (ii) Suppose that the donors are not depleted, $\tilde{n}_e \ll N_D^+ \simeq N_A \ll N_D$, a condition which is satisfied by most photorefractive materials away from saturation. (iii) Write the light intensity as in Eq. (2): $I(\mathbf{x},t) = I_0(\mathbf{x})[1 + M(\mathbf{x},t)]$, where M is a function always much smaller than unity. (iv) Use as variables n_D and n_e, the fluctuations of the charge densities around their equilibrium values, N_0^+ and n_0, for a plane wave of intensity $I_{\mathrm{PW}} = \max[I_0(\mathbf{x})]$:

$$n_D = \frac{N_D^+ - N_0^+}{n_0}, \quad N_0^+ = n_0 + N_A \simeq N_A,$$
$$n_e = \frac{\tilde{n}_e - n_0}{n_0}, \quad n_0 = \frac{sN_D}{\gamma_D N_A} I_{\mathrm{PW}},$$

where $s \equiv \alpha_D/h\nu$. Since $|M| \ll 1$ we can expect these variables to be small quantities so that the equations for the photorefractive material can be linearized.

After having applied all these points to the previous equations, we obtain a simpler model for the photorefractive material:

$$\frac{\partial n_D}{\partial t} = \frac{1}{\tau_F}[M(\mathbf{x},t) - n_e],$$

$$\frac{\partial n_e}{\partial t} - \frac{\partial n_D}{\partial t} = \frac{1}{\tau_{\mathrm{DR}}}\left(l_D^2 \nabla^2 n_e + n_D - n_e + \frac{\epsilon}{e n_0}\nabla n_e \cdot \mathbf{E}_A\right), \tag{7}$$

$$\nabla^2 \tilde{\varphi} = -\frac{e n_0}{\epsilon}(n_D - n_e),$$

where $l_D \equiv \sqrt{\epsilon k_B T/(n_0 e^2)} \simeq 10^{-6}$ m is the free-electron diffusion length, $\tau_F \equiv (\gamma_D N_A)^{-1} \simeq 10^{-7}$–$10^{-9}$ s is their lifetime, and $\tau_{\mathrm{DR}} \equiv \epsilon/(\mu e n_0) \simeq 10^0$–$10^{-3}$ s is the dielectric relaxation time. Note that the dielectric relaxation time of a photorefractive crystal depends on the light intensity (through n_0), so that different regions of the crystal have different relaxation rates. As this feature would make the problem intractable, we have supposed that the pump beam is much more intense than the resonator field and that it is roughly constant in the region where the two wave mixing interaction takes place. In other words, we have considered $I_0 \simeq I_{\mathrm{PW}}$ and have simplifyed the equations accordingly. It is important to notice that the time scales of the physical processes considered here are enormously different: the excitation of the electrons in the conduction band and their recombination with a free trap is a very fast process, its time scale being τ_F. The diffusion of the electrons is, instead, a very slow process: photorefractive materials are insulators in the dark. We will take advantage of this feature later on, in the final step of building a model for the resonator field dynamics.

The driving force in Eqs. (7) is the modulation of the light intensity $M(\mathbf{x},t)$; this term has a spatial wave vector $\mathbf{K}_{PR}$ and a temporal oscillation frequency δ_{PR}. These two quantities can be factored out from the definitions of the photorefractive variables:

$$n_D(\mathbf{x},t) = \nu_D(\mathbf{x},t)e^{i(\mathbf{K}_{PR}\cdot\mathbf{x} - \delta_{PR}t)} + \text{c.c.},$$
$$n_e(\mathbf{x},t) = \nu_e(\mathbf{x},t)e^{i(\mathbf{K}_{PR}\cdot\mathbf{x} - \delta_{PR}t)} + \text{c.c.},$$
$$\tilde{\varphi}(\mathbf{x},t) = \varphi(\mathbf{x},t)e^{i(\mathbf{K}_{PR}\cdot\mathbf{x} - \delta_{PR}t)} + \text{c.c.}$$

Note that while the spatial oscillations are "fast" ($\mathbf{K}_{PR}$ is of the same order of the pump and resonator field wave vectors) this is not true for the temporal oscillations [cf. the paragraph below Eqs. (3)]. The introduction of ν_D, ν_e, and φ allows us to simplify the problem even further. The new variables change in the same way as the resonator field amplitude F_R, i.e., on the length scale of the beam waist (typically 1 mm), while the Laplacian in Eqs. (7) is active on length scales of the order of 1 μm. Therefore the effect of the Laplacian on the new variables is negligible and we can write Eqs. (7) as

$$\frac{\partial \nu_D}{\partial t} = \frac{1}{\tau_F}\left[\frac{F_P F_R^*}{|F_P|^2+|F_R|^2} - \nu_e\right] + i\delta_{PR}\nu_D,$$

$$\frac{\partial \nu_e}{\partial t} - \frac{\partial \nu_D}{\partial t} = \frac{1}{\tau_{DR}}\Big(-l_D^2 K_{PR}^2 \nu_e + \nu_D - \nu_e + i\frac{\epsilon}{en_0}\mathbf{K}_{PR}\cdot\mathbf{E}_A\nu_e\Big) + i\delta_{PR}(\nu_e-\nu_D), \tag{8}$$

$$\varphi = \frac{en_0}{\epsilon}\frac{\nu_D-\nu_e}{K_{PR}^2},$$

where K_{PR} is the modulus of $\mathbf{K}_{PR}$. Finally we consider here the case of no external field applied to the crystal so that the second of Eqs. (8) can be replaced by

$$\frac{\partial \nu_e}{\partial t} - \frac{\partial \nu_D}{\partial t} = \frac{1}{\tau_{DR}}\left(-l_D^2 K_{PR}^2 \nu_e + \nu_D - \nu_e\right) + i\delta_{PR}(\nu_e-\nu_D).$$

The internal electric field $\mathbf{E}_I(\mathbf{x},t) = -\boldsymbol{\nabla}\tilde{\varphi}$ can be considered parallel to $\mathbf{K}_{PR}$. In fact, under the slowly-varying-amplitude approximation, the curl equation for this field becomes

$$\boldsymbol{\nabla}\times\mathbf{E}_I = \mathbf{0} \Rightarrow \mathbf{K}_{PR}\times\mathbf{E}_I \simeq \mathbf{0}$$

We can write its component in the $\mathbf{K}_{PR}$ direction, $E_I(\mathbf{x},t)$, as the product of an amplitude $\mathcal{E}_I(\mathbf{x},t)$ and a plane wave:

$$E_I(\mathbf{x},t) = \mathcal{E}_I(\mathbf{x},t)e^{i(\mathbf{K}_{PR}\cdot\mathbf{x}-\delta_{PR}t)} + \text{c.c.}$$

The value of $\mathcal{E}_I(\mathbf{x},t)$ can be obtained from the last of Eqs. (8):

$$\mathcal{E}_I(\mathbf{x},t) = -i\frac{en_0}{\epsilon}\frac{\nu_D-\nu_e}{K_{PR}}.$$

$\mathbf{E}_I(\mathbf{x},t)$ changes the index of refraction of the material via the electro-optic effect [11]:

$$\Delta n(\mathbf{x},t) = -\frac{1}{2}n_b^3 r_{\text{eff}} E_I(\mathbf{x},t) = -\frac{1}{2}n_b^3 r_{\text{eff}}\left[\mathcal{E}_I(\mathbf{x},t)e^{i(\mathbf{K}_{PR}\cdot\mathbf{x}-\delta_{PR}t)} + \text{c.c.}\right],$$

where r_{eff} is the opto-electric coefficient of the material in the direction of $\mathbf{K}_{PR}$ and n_b is the background refractive index. It is through this change of the refractive index that the resonator field is coupled to the pump beam.

III. THE FIELD EQUATION

We now turn our attention to the resonator field. We assume that the speed of light inside the photorefractive medium is c. In the Appendix we prove that this approximation is correct up to terms of the order of the ratio between the length of the photorefractive medium and the length of the cavity. As we suppose throughout this article that this ratio is very small, these corrections are negligible.

We are going to discuss the field dynamics in the framework of the empty-cavity modes, the Gauss-Laguerre modes. A complete and detailed treatment of these functions is contained in Ref. [8]. Here we just sketch the characteristics which are more relevant to our model.

For each longitudinal mode of the cavity, identified by an integer n, there is a set of transverse modes, the Gauss-Laguerre modes. These are stationary solutions of Maxwell equation in the cavity in the absence of the photorefractive medium:

$$\frac{\partial F_R}{\partial z} = \frac{i}{2K_R}\nabla^2 F_R,$$

where K_R is the modulus of the resonator field wave vector $\mathbf{K}_R$ and $\nabla_\perp^2$ is the Laplacian along the transverse coordinates. The Gauss-Laguerre modes are functions of the transverse coordinates r and φ and of the longitudinal coordinate z. They are identified by three integers: $p \geq 0$, the radial index (i.e., the number of zeros along the radial direction); $m \geq 0$, the angular index (the number of zeros in the angular direction); and i, an index that takes only two values 0 and 1. Their shape in the plane $z = 0$ (see Fig. 1) is

$$A_{\{p,m,i\}}(r,\varphi,z=0) \equiv \mathcal{A}_{pm}(r)B_m^{(i)}(\varphi) = 2(2r^2/\eta_1)^{m/2}\left[\frac{p!}{(p+m)!}\right]^{1/2} L_p^m(2r^2/\eta_1) \times e^{-r^2/\eta_1}B_m^{(i)}(\varphi),$$

where η_1 is the square of the minimum beam waist and $L_p^m(x)$ is the associated Laguerre polynomial of order p and index m:

$$L_p^m(x) = (-1)^p\sum_{n=0}^{p}\frac{(-1)^n}{n!}\binom{p+m}{p-n}x^n,$$

while

$$B_m^{(i)}(\varphi) = \begin{cases} \frac{1}{\sqrt{2\pi}} & \text{if } m=0 \\ \frac{1}{\sqrt{\pi}}\sin(m\varphi) & \text{if } m>0 \text{ and } i=0 \\ \frac{1}{\sqrt{\pi}}\cos(m\varphi) & \text{if } m>0 \text{ and } i=1. \end{cases}$$

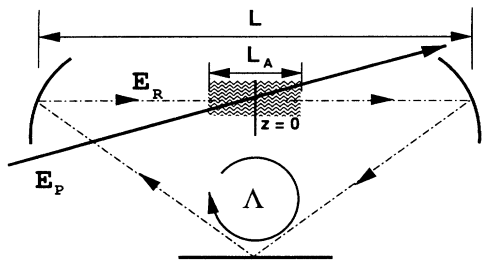

FIG. 1. Ring resonator structure. Λ is the total cavity length, E_R is the resonator field, and E_P is the pump.

Each mode has frequency of oscillation

$$\omega_{n,p,m} = \frac{2\pi c}{\Lambda} n + \frac{c}{\Lambda}(2p + m + 1)a, \tag{9}$$

where a is a parameter that depends on the cavity geometry. In the case of the cavity shown in Fig. 1, for example [8],

$$a \equiv 2\left[\tan^{-1}\left(\frac{\Lambda - L}{K_R \eta_2}\right) + \tan^{-1}\left(\frac{L}{K_R \eta_1}\right)\right],$$

where η_2 is the beam waist at $z = \Lambda/2$ (the plane mirror in Fig. 1). Two typical mode spectra are shown in Fig. 2. In the top part, (a), the spacing between longitudinal modes is much bigger than the spacing between transverse modes (nearly plane mirror cavity): each set of transverse modes is near the "parent" longitudinal mode. In the bottom part, (b), the transverse mode spacing

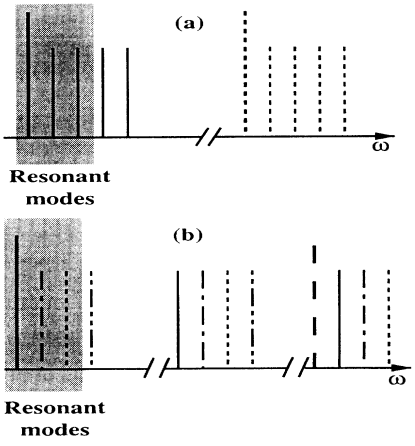

FIG. 2. Mode spectrum of a laser cavity. In (a) (nearly plane mirror cavity) the transverse-mode spacing is much smaller than the free spectral range and the transverse modes (short lines) are near their corresponding longitudinal mode (long lines). In (b) (nearly confocal cavity) the transverse modes belong to different longitudinal modes. The shaded areas indicate the modes that are relevant to the dynamics.

is nearly half of the longitudinal mode spacing (nearly confocal cavity), and the transverse modes close to each longitudinal mode have different longitudinal indices.

The total optical field in the photorefractive medium is the field $\mathcal{E}$ defined in Eq. (1); its evolution is controlled by Maxwell's equation:

$$\nabla^2 \mathcal{E}(\mathbf{x},t) - \frac{1}{c^2}\frac{\partial^2 \mathcal{E}}{\partial t^2} = \frac{2n_b \Delta n(\mathbf{x},t)}{c^2}\frac{\partial^2 \mathcal{E}}{\partial t^2}. \tag{10}$$

As stated at the beginning of Sec. II the total optical field is the sum of the pump field,

$$E_P(\mathbf{x},t) = F_P(\mathbf{x}) e^{i(\mathbf{K}_P \cdot \mathbf{x} - \omega_P t)} + \text{c.c.},$$

and the resonator field,

$$E_R(\mathbf{x},t) = F_R(\mathbf{x},t) e^{i(\mathbf{K}_R \cdot \mathbf{x} - \omega_R t)} + \text{c.c.}$$

By applying the slowly varying amplitude approximation to Eq. (10) and by decomposing $\mathcal{E}$ in F_P and F_R we obtain an equation for the resonator field amplitude:

$$2iK_R \frac{\partial}{\partial z} F_R + \frac{2i\omega_C}{c^2}\frac{\partial}{\partial t} F_R + \nabla_\perp^2 F_R$$

$$= + \frac{n_b^4 \omega_P^2}{c^2} r_{\text{eff}} \mathcal{E}_I^*(\mathbf{x},t) F_P(\mathbf{x}) + \frac{2\omega_C \delta_{CR}}{c^2} F_R, \tag{11}$$

where the z direction coincides with the cavity axis and $\nabla_\perp^2$ is the Laplacian along the transverse coordinates. The frequency $\omega_C \equiv \omega_{N,0,0}$ that appears in this equation is the frequency of the longitudinal mode N that lies nearest to the pump frequency. δ_{CR} is the frequency detuning between this cavity frequency and the unspecified reference frequency ω_R:

$$\delta_{CR} \equiv \omega_C - \omega_R.$$

Finally, K_R, the modulus of the resonator field wave vector $\mathbf{K}_R$, is defined by $K_R \equiv \omega_C/c$. At this stage, we have recast the problem in a form very similar to the laser case: we have a cavity frequency ω_C, an atomic frequency (the pump frequency) ω_P, and the resonator (laser) field oscillates at an unspecified reference frequency ω_R.

The resonator field can be decomposed along the Gauss-Laguerre basis,

$$F_R(r,\varphi,z,t) = \sum_{\{p,m,i\}} \bar{f}_{\{p,m,i\}}(z,t) A_{\{p,m,i\}}(r,\varphi,z), \tag{12}$$

and its equation [Eq. (11)] transformed in a set of partial differential equations for the mode amplitudes:

$$\frac{\partial}{\partial z}\bar{f}_{\{p,m,i\}} + \frac{1}{c}\frac{\partial}{\partial t}\bar{f}_{\{p,m,i\}}$$

$$= -\frac{i}{c}\delta_{CR}\bar{f}_{\{p,m,i\}} - i\alpha \int dr\, d\varphi\, r A^*_{\{p,m,i\}}(r,\varphi,z) \times \mathcal{E}_I^*(r,\varphi,z,t) F_P(r,\varphi,z) \tag{13}$$

where

$$\alpha \equiv \frac{n_b^4 \omega_P^2}{2K_R c^2} r_{\text{eff}}. \tag{14}$$

The advantage of decomposing the field along the empty-cavity modes is that the behavior of each mode amplitude during the propagation outside the photorefractive medium is very simple. Each mode is just phaseshifted with respect to the reference frequency ω_R and is attenuated due to losses at the mirrors. The amplitude of the $\{p,m,i\}$ mode at the right hand side of the photorefractive medium is transformed by the propagation in the cavity so that its value at the left of the photorefractive crystal is

$$\bar{f}_{\{p,m,i\}}(-\tfrac{1}{2}L_A,t) = Re^{-i\delta_{pm}} e^{-i\delta_{CR}(\Lambda-L_A)/c} \times \bar{f}_{\{p,m,i\}}\left(\frac{1}{2}L_A, t-\frac{\Lambda-L_A}{c}\right), \tag{15}$$

where R is the total mirror reflectivity and $\delta_{pm} \equiv (2p+m)a$. We now introduce these boundary conditions into the field equation. The standard procedure for doing this is to define a new time variable and new amplitudes:

$$\begin{aligned} t' &= t + \frac{\Lambda - L_A}{c}\left(\frac{z}{L_A}+\frac{1}{2}\right) \Rightarrow \frac{\partial}{\partial t} = \frac{\partial}{\partial t'}, \\ z' &= z \Rightarrow \frac{\partial}{\partial z} = \frac{\partial}{\partial z'} + \frac{\Lambda - L_A}{L_A c}\frac{\partial}{\partial t'}, \end{aligned} \tag{16}$$

$$\tilde{f}_{\{p,m,i\}}(z',t') = \exp\left\{\left[\ln R - i\delta_{CR}\frac{\Lambda-L_A}{c} - i\delta_{pm}\right]\left(\frac{z'}{L_A}+\frac{1}{2}\right)\right\} \times \bar{f}_{\{p,m,i\}}(z',t'). \tag{17}$$

The purpose of these definitions is to move the field dynamics outside the medium into the medium itself: suppose that the field $\bar{f}_{\{p,m,i\}}$ does not change inside the medium. Then the field $\tilde{f}_{\{p,m,i\}}$ changes across the slice exactly as the field $\bar{f}_{\{p,m,i\}}$ changes during propagation in the cavity. This is the main reason why we must suppose that the dynamics of the original field $\bar{f}_{\{p,m,i\}}$ inside the medium is very simple; more general cases would produce unworkable equations.

Since the dynamics outside the medium is taken into account in the definition of $\tilde{f}_{\{p,m,i\}}$, the boundary condition on these variables are extremely simple:

$$\tilde{f}_{\{p,m,i\}}(-\tfrac{1}{2}L_A,t') = \tilde{f}_{\{p,m,i\}}(\tfrac{1}{2}L_A,t'). \tag{18}$$

Their equation, however, is far from simple:

$$\frac{\partial}{\partial z'}\tilde{f}_{\{p,m,i\}} + \frac{\Lambda}{L_A c}\frac{\partial}{\partial t'}\tilde{f}_{\{p,m,i\}} - \left[\ln R - i\delta_{CR}\frac{\Lambda}{c} - i\delta_{pm}\right]\frac{1}{L_A}\tilde{f}_{\{p,m,i\}} = -i\alpha \exp\left\{\left[\ln R - i\delta_{CR}\frac{\Lambda-L_A}{c} - i\delta_{pm}\right]\left(\frac{z'}{L_A}+\frac{1}{2}\right)\right\} \int dr\, d\varphi\, r\mathcal{E}_I^*(r,\varphi,z',t)F_P(r,\varphi,z')A^*_{\{p,m,i\}}(r,\varphi,z'). \tag{19}$$

We use the boundary condition, Eq. (18), to eliminate the z derivative by expanding the amplitudes $\tilde{f}_{\{p,m,i\}}(z',t')$ in longitudinal modes:

$$\tilde{f}_{\{p,m,i\}}(z',t') = \sum_n \hat{f}_{\{n,p,m,i\}}(t')e^{i2\pi(n-N)(z'/L_A+1/2)}.$$

Note that these modes automatically satisfy the boundary conditions (18). We have to write the factor $(n-N)$ in the exponential because we have already taken into account the longitudinal dependence of the reference mode $\{N,0,0\}$ while writing Eq. (11). Equation (19) now becomes

$$\frac{\Lambda}{L_A c}\frac{\partial}{\partial t'}\hat{f}_{\{n,p,m,i\}} - \left[\ln R - i\delta_R^{(n)}\frac{\Lambda}{c} - i\delta_{pm}\right]\frac{1}{L_A}\hat{f}_{\{n,p,m,i\}} = -i\alpha\int_{-L_A/2}^{L_A/2} dz' \exp\left\{\left[\ln R - i\delta_R^{(n)}\frac{\Lambda-L_A}{c} - i\delta_{pm}\right]\left(\frac{z'}{L_A}+\frac{1}{2}\right)\right\} \times \int dr\, d\varphi\, r\mathcal{E}_I^*(r,\varphi,z',t)F_P(r,\varphi,z')A^*_{\{p,m,i\}}(r,\varphi,z') \tag{20}$$

where $\delta_R^{(n)} \equiv \omega_{n00} - \omega_R$ is the frequency detuning between the longitunal mode n and the reference frequency ω_R.

We now apply the mean-field limit to this equation. We suppose that the losses in the cavity are small so that only the modes that are "near" the pump frequency are excited (shaded areas in Fig. 2). As the output from the resonator is a finite quantity, we must suppose that also the gain per single pass is a very small quantity, of the order of the losses. More formally, we take the transmittivity of the mirrors $T_M \equiv 1 - R$ as smallness parameter. We require the gain [the right-hand side of Eq. (20)] to be of the same order of magnitude as T_M. The request, stated above, that only the modes whose frequency is near the pump frequency are active, means,

in a more formal way, that the phase shift during propagation caused by the difference between the active modes frequencies and ω_R is a quantity of order T_M. This can be taken as a definition for the term "resonant modes" used in Fig. 2: the resonator field is the sum of the transverse modes whose frequency difference with respect to the pump frequency (note that $\omega_P \simeq \omega_R$) is of the order of the cavity line width:

$T_M \ll 1$ (smallness parameter),

$$|\omega_{n,p,m} - \omega_R|\frac{\Lambda}{c} \simeq O(T_M) \ll 1$$

(detuning $\ll$ free spectral range),

$\alpha|\mathcal{E}_I|L_A \simeq O(T_M) \ll 1$ (mean-field limit).

We now expand Eq. (20) to first order in T_M. A consequence of all these hypotheses is that we can approximate the exponential with 1. Always in the spirit of the mean field limit, we require that the pump is not depleted in the medium (the gain per single pass is small), so that neither F_P nor $\mathcal{E}_I$ depends on z'. Finally, we suppose that the length of the active medium is much larger than the Rayleigh range of the cavity so that the Gauss-Laguerre modes do not change appreciably in it: $A_{\{p,m,i\}}(r,\varphi,z') \simeq A_{\{p,m,i\}}(r,\varphi,0)$. The final result is a set of ordinary differential equations for the modal amplitudes:

$$\frac{d}{dt'}\hat{f}_{\{n,p,m,i\}} = -\kappa\Big\{ [1 + i\Delta_R^{(n)} + i\tilde{a}(2p+m)]\hat{f}_{\{n,p,m,i\}} + i2C\int dr\, d\varphi\, r\mathcal{E}_I^*(r,\varphi,t) \times F_P(r,\varphi)A^*_{\{p,m,i\}}(r,\varphi)\Big\} \tag{21}$$

where

$$\kappa = \frac{cT_M}{\Lambda}, \quad \Delta_R^{(n)} \equiv \frac{\delta_R^{(n)}\Lambda}{cT_M},$$
$$\tilde{a} \equiv \frac{a}{T_M}, \quad 2C \equiv \frac{\alpha L_A}{T_M}.$$

In the case where all the transverse modes belong to the same longitudinal mode ($a \ll \pi$) we can write the equation for the electric field as a single partial differential equation rather than as a set of ordinary differential equations for the mode amplitudes. In this case, in fact, we can write the field as the sum over all the transverse modes of a chosen longitudinal mode N [8]:

$$F_R(r,\varphi,z',t') = \sum_{\{p,m,i\}} \hat{f}_{(p,m,i)}(t')A_{(p,m,i)}(r,\varphi)$$

and use the property of the Gauss-Laguerre modes

$$\left(\frac{\eta_1}{4}\nabla_\perp^2 + 1 - \frac{r^2}{\eta_1}\right)A_{(p,m,i)} = -(2p+m)A_{(p,m,i)}$$

to sum the entire set of Eq. (21) and obtain

$$\frac{\partial F_R}{\partial t'} = -\kappa\Big\{ \left[1 + i\Delta_{CR} - i\tilde{a}\left(\eta_1\frac{\nabla_\perp^2}{4} + 1 - \frac{r^2}{\eta_1}\right)\right]F_R + i2CF_P(r,\varphi)\mathcal{E}_I^*(r,\varphi,t')\Big\},$$

where $\Delta_{CR} \equiv \Delta_R^{(N)} = \delta_{CR}\Lambda/(cT_M)$.

IV. THE MODEL'S EQUATION

We have now built the two main blocks of our model: the equation for the photorefractive material, Eqs. (8), and those for the resonator field, Eqs. (21). What we still have to do is to put together the two sets of equations, further simplify the model by making use of the fact that one time scale τ_{DR} is much longer than the other two τ_F and $1/\kappa$, and finally discuss the hypotheses which are at the base of this model.

As stated in Sec. III we suppose that the pump and the resonator field do not change appreciably in the material, so that we can neglect any z dependence in the resonator and in the material equations [Eqs. (21) and (8), respectively]. Finally, the difference between t and t' is of the order of the slice thickness and, therefore, is negligible:

$$\frac{\partial \nu_D}{\partial t} = \frac{1}{\tau_F}\left[\frac{F_P F_R^*}{|F_P|^2 + |F_R|^2} - \nu_e\right] + i\delta_{PR}\nu_D,$$
$$\frac{\partial \nu_D}{\partial t} - \frac{\partial \nu_e}{\partial t} = -\frac{1}{\tau_{DR}}(\nu_D - \nu_e - C_D\nu_e) + i\delta_{PR}(\nu_D - \nu_e), \tag{22}$$

$$\frac{d}{dt}\hat{f}_{\{n,p,m,i\}} = -\kappa\Big\{ [1 + i\Delta_R^{(n)} + i\tilde{a}(2p+m)]\hat{f}_{\{n,p,m,i\}} - C_{PR}\int dr\, d\varphi\, rF_P(r,\varphi)(\nu_D^* - \nu_e^*) \times A^*_{\{p,m,i\}}(r,\varphi)\Big\},$$

$$F_R(r,\varphi,t) = \sum_{\{n,p,m,i\}} \hat{f}_{\{n,p,m,i\}}(t)A_{\{p,m,i\}}(r,\varphi),$$

where

$$C_D \equiv l_D^2 K_{PR}^2 = \frac{K_B T\epsilon}{n_0 e^2}K_{PR}^2$$

is a dimensionless parameter which measures the efficiency of diffusion in the photorefractive material, while

$$C_{PR} \equiv 2C\frac{en_0}{\epsilon K_{PR}} = \frac{n_b^4\omega_P^2}{2K_R T_M v^2}L_A r_{\text{eff}}\frac{en_0}{\epsilon K_{PR}}$$

is a dimensionless parameter which measures the coupling strength between the pump and resonator fields.

We are now ready for the final step: the time scale of the second of Eqs. (22) is much longer than those of the first and third equations. We can adiabatically eliminate these latter equations and reduce the model even further. Keeping in mind that $\delta_{PR}\tau_F \ll 1$ [we will show later that $\delta_{PR}\tau_{DR} \simeq O(1)$, Eq. (25)], we obtain from the first of Eqs. (22)

$$\nu_e = \frac{F_P F_R^*}{|F_P|^2 + |F_R|^2}.$$

From the third equation we obtain

$$\hat{f}_{\{n,p,m,i\}} = \frac{C_{PR}}{1 + i\Delta_R^{(n)} + i\tilde{a}(2p+m)} \times \mathcal{P}_{\{p,m,i\}}[F_P(r,\varphi)(\nu_D^* - \nu_e^*)],$$

where $\mathcal{P}_{\{p,m,i\}}$ is the projection operator onto the $\{p,m,i\}$ Gauss-Laguerre mode. This last equation can be put into the second of Eqs. (22):

$$\frac{d}{d\bar{t}}\hat{f}_{\{n,p,m,i\}}(\bar{t}) = -\left[(1 + i\Delta_{PR})\hat{f}_{\{n,p,m,i\}}(\bar{t}) - \frac{B}{1 + i\Delta_R^{(n)} + i\tilde{a}(2p+m)} \times \mathcal{P}_{\{p,m,i\}}\left(\frac{|F_P|^2 F_R}{|F_P|^2 + |F_R|^2}\right)\right]$$

where $\bar{t} = t/\tau_{DR}$, $\Delta_{PR} \equiv \delta_{PR}\tau_{DR}$, and $B \equiv C_D C_{PR}$. The coefficient B measures the efficiency of the energy transfer between pump and resonator field and plays in this model the same role as the pump intensity in a homogeneously broadened laser equation [8]. We will see later that B is the bifurcation parameter for the resonator field threshold. Finally, we can scale the pump intensity (but not its shape) from this equation. We can define

$$I_P = \max[F_P(r,\varphi)], \quad F_P(r,\varphi) \equiv \sqrt{I_P}F_{\mathcal{P}}(r,\varphi),$$
$$F_R(r,\varphi,\bar{t}) \equiv \sqrt{I_P}F_{\mathcal{R}}(r,\varphi,\bar{t}),$$
$$\hat{f}_{\{n,p,m,i\}} = \sqrt{I_P}f_{\{n,p,m,i\}},$$

and write

$$\frac{d}{d\bar{t}}f_{\{n,p,m,i\}}(\bar{t}) = -\left[(1 + i\Delta_{PR})f_{\{n,p,m,i\}}(\bar{t}) - \frac{B}{1 + i\Delta_R^{(n)} + i\tilde{a}(2p+m)} \times \mathcal{P}_{\{p,m,i\}}\left(\frac{|F_{\mathcal{P}}|^2 F_{\mathcal{R}}}{|F_{\mathcal{P}}|^2 + |F_{\mathcal{R}}|^2}\right)\right]. \tag{23}$$

These equations, one for each active Gauss-Laguerre mode, are the final result of this section. They are relatively simple: the integral can be evaluated numerically in a very efficient manner and there are plenty of reliable algorithms for integrating large systems of ordinary differential equations. On the other hand, they have been obtained by making many assumption on the behavior of the photorefractive material and of the field. First of all, we have linearized the equations for the photorefractive material. This hypothesis is not very stringent: in Ref. [12] it is shown that the linear approximation is good even for modulation of the input intensity of the order of 50%. The most stringent assumption that we had to make is that the slice of photorefractive material is very thin: as a consequence neither the pump beam nor the resonator field changes significantly in it and absorption in the material can be neglected. This last point is very important. The mean-field-limit approximation can be made only under the hypothesis that losses in the cavity are small and that the field does not change significantly in the photorefractive medium.

There are other two points that should be clarified: the first is the use of the Gauss-Laguerre modes to decompose the resonator field. It has been shown numerically in Ref. [14] that the Gauss-Laguerre modes are a good basis onto which to decompose the laser field in a resonator with spherical mirrors, provided that the pump is not narrower than the beam waist. The second one is the adiabatic elimination of the two fast equations. In Ref. [15] it has been shown that the adiabatic elimination of fast variables in models which involve spatial coordinates can give rise to spurious results. This is due to the fact that different length scales may have different time scales. This is not the case in our model: long wavelengths evolve with a time scale of $1/\kappa$, i.e., they are "fast" variables and can be eliminated. Short wavelengths evolve on a scale that is even faster and so pose no problem.

V. STATIONARY STATES AND THEIR STABILITY

Finding the stationary states of Eq. (23) is not a trivial task. It can be made somewhat simpler if we suppose that the equilibrium configuration of the field is a pure Gaussian mode,

$$F_R = f_{\{n,0,0\}}A_{0,0}(\rho,\varphi) = f_{\{n,0,0\}}\sqrt{\frac{2}{\pi}}e^{-\rho^2},$$

where $\rho^2 = r^2/\eta_1$ is the radial variable r scaled to the beam waist. This is, of course, an approximation. The Gaussian mode feeds energy through the projection operator to all the modes $\{p,0\}$. However, if the intermode spacing is not too small and if we are close to threshold, the approximation holds quite well.

Putting this function into Eq. (23) we obtain an implicit relation between the stationary mode intensity $f_{(0)}$ and the model's parameters

$$\frac{1 + (\Delta_R^{(n)})^2}{B} = \int_0^\infty dx \frac{e^{-x}}{1 + \frac{2}{\pi}|f_{(0)}|^2 e^{-x(1-1/w^2)}}, \tag{24}$$

$$\Delta_{PR} = -\Delta_R^{(n)}, \tag{25}$$

where $x \equiv 2\rho^2$. We have supposed that the pump has a Gaussian shape, $\mathcal{F}_\mathcal{P} = e^{-\rho^2/w^2}$, with spot size w. Note that Eq. (25) is analogous to the typical mode-pulling equation of laser physics. The equation for the amplitude can be solved analytically if we assume that the intensity of the Gaussian mode is very small, $|f_{(0)}|^2 \ll \pi/2$. This limit is coherent with the hypothesis that the stationary solution is a pure Gaussian mode; as stated at the beginning of this section, if the intensity of the resonator field is very high it is unreasonable to suppose that only the Gaussian mode is excited. If we Taylor expand the denominator we can evaluate the integral and obtain

$$|f_{(0)}|^2 \simeq \frac{\pi}{2}\left(2 - \frac{1}{w^2}\right)\left(1 - \frac{1 + (\Delta_R^{(n)})^2}{B}\right). \tag{26}$$

As expected, the threshold value of B is higher the larger the detuning: the Gaussian mode is active only if $B > [1 + (\Delta_R^{(n)})^2]$. Furthermore, its intensity depends on the overlap between the pump and the Gaussian mode: it is higher for broader pumps.

We now investigate the stability of this solution. We can write the resonator field as the sum of this stationary solution plus a small perturbation:

$$F_\mathcal{R} = F_0 + \sum_{\{p,m,i\}} \delta f_{\{p,m,i\}} A_{\{p,m,i\}},$$

where $F_0 \equiv f_{(0)} A_{\{0,0\}}$. We have dropped the index of the longitudinal mode for ease of notation. Equation (23), linearized around the stationary solution F_0, becomes

$$\frac{d}{dt}\delta f_{\{p,m,i\}} = -\Bigg\{(1 + i\Delta_{PR})\delta f_{\{p,m,i\}} - \frac{B}{1 + i[\Delta_R^{(n)} + \tilde{a}(2p+m)]} \times \Bigg[\mathcal{P}_{\{p,m,i\}}\left(\frac{|F_\mathcal{P}|^4}{(|F_\mathcal{P}|^2 + |F_0|^2)^2}\sum_{\{\alpha,\beta,\gamma\}} \delta f_{\{\alpha,\beta,\gamma\}} A_{\{\alpha,\beta,\gamma\}}\right) - \mathcal{P}_{\{p,m,i\}}\left(\frac{|F_\mathcal{P}|^2 F_0^2}{(|F_\mathcal{P}|^2 + |F_0|^2)^2}\sum_{\{\alpha,\beta,\gamma\}} \delta f^*_{\{\alpha,\beta,\gamma\}} A^*_{\{\alpha,\beta,\gamma\}}\right)\Bigg]\Bigg\}.$$

We restrict our attention to the first three modes: the Gaussian $\{0,0\}$ and the two (doughnut) modes $\{0,1,0\}$ and $\{0,1,1\}$. For symmetry reasons the Gaussian is not coupled to the two doughnut modes and its equation is irrelevant to the study of the stability of the stationary solution. The other four equations (for each mode there is an equation for the amplitude and its complex conjugate) split in two identical blocks, as each mode is coupled only to its complex conjugate. The equation for the perturbation along the $\{0,1,0\}$ mode, $\delta f_{\{0,1,0\}} \equiv \delta f_1$ is

$$\begin{aligned}\frac{d}{dt}\delta f_1 &= -\Bigg[(1 + i\Delta_{PR})\delta f_1 - \frac{B}{1 + i(\Delta_R^{(n)} + a)}(C_1\delta f_1 - C_2\delta f_1^*)\Bigg],\\ \frac{d}{dt}\delta f_1^* &= -\Bigg[(1 - i\Delta_{PR})\delta f_1^* - \frac{B}{1 - i(\Delta_R^{(n)} + a)}(C_1\delta f_1^* - C_2\delta f_1)\Bigg],\end{aligned} \tag{27}$$

where

$$C_1 = \int_0^\infty dx \frac{xe^{-x}}{\left(1 + \frac{2}{\pi}|f_{(0)}|^2 e^{-x(1-1/w^2)}\right)^2},$$

$$C_2 = \frac{2}{\pi}|f_{(0)}|^2 \int_0^\infty dx \frac{xe^{-x(2-1/w^2)}}{\left(1 + \frac{2}{\pi}|f_{(0)}|^2 e^{-x(1-1/w^2)}\right)^2}.$$

Note that we have considered $f_{(0)}$ to be real. However, this assumption is not strictly needed, it just simplifies the notation.

The perturbation can be written as

$$\begin{pmatrix}\delta f_1(t)\\ \delta f_1^*(t)\end{pmatrix} = e^{\lambda t}\begin{pmatrix}\delta f_1^{(0)}\\ \delta f_1^{(0)*}\end{pmatrix}.$$

Putting this expression into Eqs. (27) we obtain a system of algebraic equations with eigenvalues

$$\lambda = D_1 - 1 \pm \sqrt{D_2^2[1 + (\Delta_R^{(n)} + a)^2] - [\Delta_{PR} + D_1(\Delta_R^{(n)} + a)]^2}$$

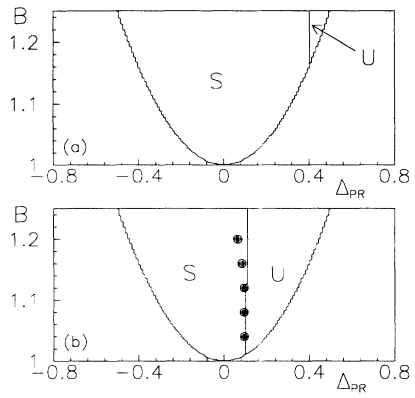

FIG. 3. Stability region for the Gaussian mode: the gaussian solution is stable in the region marked S and unstable in that marked U. For parameter values in the region below the lower parabola the Gaussian solution is below threshold. The dots show the boundary of instability obtained from numerical simulations. $\tilde{a}$ has value 0.2 (top) or 0.8 (bottom). The pump width is $w = 5.0$ and $\Delta_{PR} = -\Delta_R^{(n)}$ in both cases.

where

$$D_1 \equiv \frac{BC_1}{1+(\Delta_R^{(n)}+a)^2}, \quad D_2 \equiv \frac{BC_2}{1+(\Delta_R^{(n)}+a)^2}.$$

The stationary Gaussian solution is stable if the eigenvalues of this equations have negative real parts. For small field intensities, we can use Eq. (26), and obtain

$$\mathrm{Re}(\lambda) \simeq -\frac{2a\Delta_R^{(n)}+a^2}{1+(\Delta_R^{(n)}+a)^2}.$$

The most striking aspect of this relation is that the stability is independent of the pump parameter B. This characteristic continues to be valid also for larger values of the resonator field intensity (see Fig. 3). In the case of larger transverse-mode spacing [Fig. 3(a)] the Gaussian solution is stable over a wide region; if the modes are closer one to the other [Fig. 3(b)] the region of stability shrinks.

We have tested these results by integrating Eq. (23) on the boundary of instability (see Sec. VI for a description of the numerical method used). The numerical boundary is shifted to the left with respect to the theoretical one [large circles in Fig. 3(b)]. This effect is probably due to the fact that the stationary solution is not a pure Gaussian one. As an example, the intensity of the $\{1,0\}$ mode is 5% of the intensity of the Gaussian mode for the parameter values of the top circle in Fig. 3(b).

VI. NUMERICAL ANALYSIS

The analytical results obtained in the preceding section are a map to the model dynamics. Unfortunately it is very difficult to obtain analytical information on the existence, stability, and general properties of any other asymptotic state. Therefore we have written a computer program that integrates Eqs. (23) and we have run many simulations with different parameter values and initial conditions.

In all our simulations we have supposed that the pump has a Gaussian shape, $F_{\mathcal{P}}(\rho) = \exp(-\rho^2/w^2)$, and that the cavity has nearly plane mirrors so that the transverse modes all belong to a single longitudinal mode [Fig. 2(a)]. In order to write a more efficient numerical code we have preferred to use complex Gauss-Laguerre modes. The difference with those defined in Sec. III is that m can be positive or negative so that there is no need for the fourth index i. The $B_m(\varphi)$ functions are defined as

$$B_m(\varphi) = \frac{1}{\sqrt{2\pi}} e^{im\varphi}.$$

We have integrated 55 modes from $q \equiv (2p+|m|) = 0$ to $q = 9$; modes with the same q have the same frequency of oscillation, see Eq. (9), and we say that they belong to the same family. All modes have losses 1 except the modes with $p = 4$ (the highest value of the radial index such that $q \leq 9$): in order to simulate the effect of an aperture these modes have losses 10, i.e., the linear term in Eq. (23) is $(10 + i\Delta_{PR})$ instead of the customary $(1 + i\Delta_{PR})$. We must stress that this is a very rough approximation of an aperture (for a more refined method see Ref. [16]). However, choosing different losses for different modes is not a relevant feature for these simulations: the families of modes which are excited are selected by the detuning and by the strength of the coupling between the pump and resonator field. We have always checked in our simulations that no mode with $q \geq 8$ is excited. In this way we are sure that the dynamics observed is not influenced by the arbitrary truncation of the number of modes. Finally, the initial amplitudes of the Gauss-Laguerre modes were always chosen randomly.

The integration routine is split in two parts. The first step evaluates the projection integral. The choice of complex modes has allowed us to use a fast Fourier transform routine to integrate over the angular variable. The different Fourier components correspond to different values of index m. The integration over the radius is evaluated, instead, with a Gauss algorithm of order 15, a procedure that gives the exact value of the integral if the integrand is a polynomial of order less than 30. Once the projection integral has been evaluated the remaining system of ordinary differential equations has been integrated via a variable-step variable-order algorithm. The final program is very fast: the integration of 55 Gauss-Laguerre modes for two hundred units of time takes roughly 10 min on a Sun SparcStation 1. We have checked the correctness of our simulations by comparing some results with simulations performed with either different accuracy in the temporal integration algorithm or different order in the Gauss integration method.

The control parameters are the transverse mode spacing $\tilde{a}$, the pump-field detuning Δ_{PR}, and the energy transfer coefficient B. The values of B must be slightly larger than one for the linearization hypothesis to be correct; higher values give a resonator field intensity that is

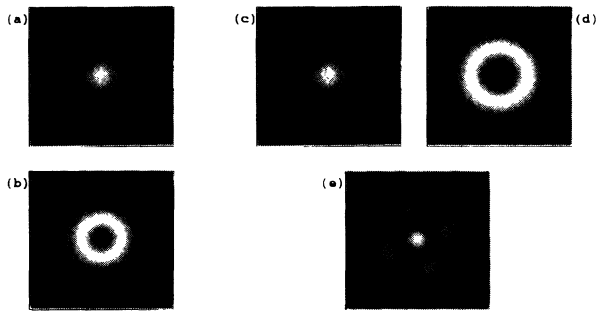

FIG. 4. Transverse-mode images: in these simulations $\tilde{a}$ is sufficiently large so that the pump is in resonance with only one family of transverse modes at a time. Gray scale, images of the intensity of the resonator field; white codes, high intensity; black, low intensity. $B = 1.4$, $\tilde{a} = 1.0$, $w = 5.0$. (a) $\Delta_{PR} = 0.0$, (b) $\Delta_{PR} = 1.0$, (c)–(e) $\Delta_{PR} = 2.0$.

far too high with respect to the pump beam. The typical value that we have used is $B = 1.1$, even though we have run some simulation with higher values of this parameter to check if anything peculiar or interesting would happen. Finally, we have chosen as reference frequency for our simulation the mode pulled frequency of the resonator field, i.e., we have chose ω_R such that $\Delta_{PR} = -\Delta_R^{(n)}$.

The most important feature that we have found is that the dynamics is very similar to that of an homogeneously broadened laser [17–19]. We have observed simple patterns, formed by a single Gauss-Laguerre mode; more complicated stationary patterns, analogous to the phase singularities crystals of Ref. [17]; and periodic patterns of rotating vortices, such as those observed in Refs. [18, 19]. There is, however, a difference of great importance: the time scale. The time scale of the dynamics in the transverse plane of a laser field is of the order of the light frequency; the time scale of the resonator field in this model is the dielectric relaxation time of the crystal τ_{DR}. As photorefractive materials are insulators, τ_{DR} is of the order of the second. In very informal terms we could say that the crystal acts as a "time expander." Here lies perhaps the greatest advantage of the resonator model that we have described in this paper: it is a very convenient tool to study simple vortex patterns.

As in the laser case the final state depends on the initial

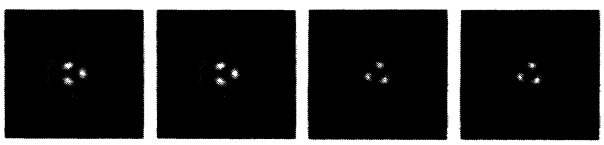

FIG. 5. Limit cycle of the resonator field. Gray scale, images of the intensity of the resonator field; white codes, high intensity; black, low intensity. The time interval between two successive images is 20. Time increases form left to right. $B = 1.1$, $\tilde{a} = 0.1$, $w = 5.0$, $\Delta_{PR} = 0.2$.

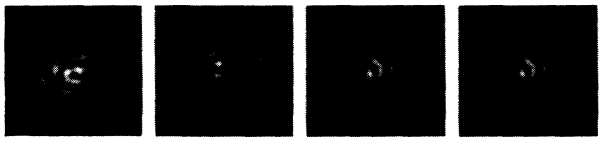

FIG. 6. Chaotic evolution of the resonator field. Gray scale images of the intensity of the resonator field, white codes high intensity, black low intensity. The time interval between successive images is 5. Time increases from left to right. $B = 1.8$, $\tilde{a} = 0.15$, $w = 5.0$, $\Delta_{PR} = 0.6$.

condition [18, 19]: for the same parameter values it is possible to obtain different final states by just starting from different initial conditions. Again as in the laser case, the dynamics is strongly dependent on the number of active modes: for small values of B and big values of the transverse mode spacing $\tilde{a}$, the pump is resonant with just one family of transverse mode at a time (see Fig. 4). By changing the value of the detuning we can obtain a Gaussian [$\{p, m\} = \{0, 0\}$] mode, a vortex of charge ± 1 [the $\{p, m\} = \{0, \pm 1\}$ modes], the $\{p, m\} = \{1, 0\}$, $\{p, m\} = \{0, \pm 2\}$ modes, or some combination of these. The pattern at bottom right [Fig. 4(e)] is analogous to the phase singularity crystals of Ref. [17]. In this case there are four vortices, two of charge +1 and two of charge -1, whose positions correspond to the dark spots of the intensity image and are fixed in space.

If the transverse mode spacing is decreased, then more families of modes are resonant with the pump beam and the pattern becomes more complicated: some of the final states of the system are limit cycles. In Fig. 5 we show the light intensity pattern for one such final state: the rotating pattern is the superposition of four different Gauss-Laguerre modes, oscillating at two different frequencies. The beat between them causes the rotation.

To conclude this section we include as a "curiosity" the images of a chaotic pattern, Fig. 6. The value of the resonator field in this simulation is greater than the pump field, a clear indication that the model hypothesis have failed. In this simulation roughly twenty modes are active and the interplay between their different oscillation frequencies produces a chaotic dynamics. Our feeling is that even though the model that we have analyzed is not capable of giving a correct description of the dynamics for these parameter values, it shows that the chaotic dynamics observed, e.g., in the experiment of Ref. [4], can be explained by the interplay of a limited number of modes.

VII. CONCLUSION

The model described in this article is an attempt to obtain a simple set of equations for the dynamics of the resonator field. This aim has been achieved: the final equations are relatively simple and can be integrated numerically without much effort. The dynamical evolution that can be observed in the numerical simulations is reminiscent of laser dynamics, with its vortex patterns, phase

singularity crystals, and turbulent states. At variance with ordinary lasers, the dynamics time scale is very slow: it is the dielectric relaxation time of the crystal, a quantity than can easily be of the order of 1 s. This makes detection and measurement of these patterns a relatively easy task in an experiment [4, 5].

On the other hand, there are many aspects of the model that we have not considered: the effect of an applied voltage on the photorefractive crystal, large angles between pump beam and resonator axis, and the higher-order gratings inside the crystal itself. We have neglected all changes in the pump and resonator field inside the crystal. All these effects may be relevant for a given experimental configuration and ought to be taken into account. They could, for example, give rise to a nonaxially symmetric gain which would favor some field configurations while increasing the losses of other modes. The mean-field approximation is probably not able to describe these effects, but we feel this is an area worth exploring.

ACKNOWLEDGMENTS

I wish to thank G.-L.Oppo for his help and for having carefully read this manuscript. This work was partially supported by SERC (Gr/F 12665) and by the EEC through a SCIENCE grant.

APPENDIX: EFFECT OF THE REFRACTIVE INDEX ON THE MEAN-FIELD LIMIT

In the derivation of the field equations (Sec. III) we have supposed that the refractive index of the active medium is one. This hypothesis is hardly realistic for photorefractive materials, as their indices of refraction are typically between two and three. In this appendix, we show that this approximation, however, is very good, again provided that the length of the active medium is much smaller than the cavity length.

We shall indicate the speed of light in the active medium with the symbol v. Moreover, throughout this appendix we shall continuously reference the corresponding paragraphs in Sec. III, in order to show where the main differences between the two approaches are.

The first step is to define Gauss-Laguerre modes for a cavity in which a region from $z=-L_A/2$ to $L_A/2$ has index of refraction n_b, while the rest of the cavity has index one. This means that we must solve the equation

$$\frac{\partial F_R}{\partial z}=\frac{i}{2K_R^{(M)}}\nabla^2 F_R$$

in the medium ($K_R^{(M)}\equiv\omega_c/v$) and the equation

$$\frac{\partial F_R}{\partial z}=\frac{i}{2K_R}\nabla^2 F_R$$

in the rest of the cavity (remember that $K_R\equiv\omega_c/c$). This problem involves very lengthy and tedious algebra: the final result is that the "new" Gauss-Laguerre modes are the same as those described in Sec. III, in the limit $L_A/\Lambda\to 0$ (Λ is the total cavity length). This can be most easily seen by the following argument: propagation in a medium of length L_A and refractive index $n_b\neq 1$ is equivalent to free-space propagation over a distance $L_{\rm eff}=n_bL_A$. Thus the "new" Gauss-Laguerre modes are the empty cavity modes of a system like the one in Fig. 1, but with an intermirror distance $L+L_A(n_b-1)$.

The second step involves the field equation. The Maxwell equation for the resonator field in the active medium (11) is

$$2iK_R^{(M)}\frac{\partial}{\partial z}F_R+\frac{2i\omega_C}{v^2}\frac{\partial}{\partial t}F_R+\nabla_\perp^2 F_R$$

$$=+\frac{n_b^4\omega_P^2}{c^2}r_{\rm eff}\mathcal{E}_I^*(\mathbf{x},t)F_P(\mathbf{x})+\frac{2\omega_C\delta_{CR}}{v^2}F_R.$$

We can expand this equation onto the set of the "new" Gauss-Laguerre modes, Eq. (12), and write the equation for the mode amplitudes [Eq. (13)]:

$$\frac{\partial}{\partial z}\bar f_{\{p,m,i\}}+\frac{1}{v}\frac{\partial}{\partial t}\bar f_{\{p,m,i\}}$$

$$=-\frac{i}{v}\delta_{CR}\bar f_{\{p,m,i\}}-i\alpha\int dr\,d\varphi\,r A^*_{\{p,m,i\}}(r,\varphi,z)\times\mathcal{E}_I^*(r,\varphi,z,t)F_P(r,\varphi,z)$$

where α is defined as in Eq. (14). As the field equation in the cavity has not changed, the boundary conditions for the mode amplitudes are still given by Eq. (15). Following the procedure described in Sec. III, we then proceed to introduce the new variables z' and t' [Eq. (16)] and the new field $\tilde f_{\{p,m,i\}}$ [Eq. (17)]. The boundary conditions for the new amplitudes are those specified in Eq. (18), while the field equation, Eq. (19), is slightly different:

$$\frac{\partial}{\partial z'}\tilde f_{\{p,m,i\}}+\left(\frac{\Lambda-L_A}{L_Ac}+\frac{1}{v}\right)\frac{\partial}{\partial t'}\tilde f_{\{p,m,i\}}-\left[\ln R-i\delta_{CR}\left(\frac{\Lambda-L_A}{c}+\frac{L_A}{v}\right)-i\delta_{pm}\right]\frac{1}{L_A}\tilde f_{\{p,m,i\}}$$

$$=-i\alpha\exp\left\{\left[\ln R-i\delta_{CR}\frac{\Lambda-L_A}{c}-i\delta_{pm}\right]\left(\frac{z'}{L_A}+\frac{1}{2}\right)\right\}\int dr\,d\varphi\,r\mathcal{E}_I^*(r,\varphi,z',t)F_P(r,\varphi,z')A^*_{\{p,m,i\}}(r,\varphi,z').$$

The difference between this equation and the equation obtained by supposing that the refractive index of the material is $n_b=1$, Eq. (19), is the coefficient of the time derivative and of the detuning

$$\frac{\Lambda - L_A}{L_A c} + \frac{1}{v}$$

instead of

$$\frac{\Lambda}{L_A c}.$$

Such a difference can be made as small as we like by considering a sufficiently short photorefractive medium.

---

* Also at Department of Physics, Heriot-Watt University, Edinburgh, Scotland.

[1] H. Rajbenbach and J.P. Huygnard, Opt. Lett. **10**, 137 (1985).
[2] J. de la Tocnaye, P. Fellat-Finet, and J.P. Huignard, J. Opt. Soc. Am. B **3**, 315 (1986).
[3] G. Pauliat and P. Günter, Opt. Commun. **66**, 329 (1988).
[4] F.T. Arecchi, G. Giacomelli, P. Ramazza, and S. Residori, Phys. Rev. Lett. **65**, 2531 (1990).
[5] F.T. Arecchi, G. Giacomelli, P. Ramazza, and S. Residori, Phys. Rev. Lett. **67**, 3749 (1991).
[6] A. Yariv and S.-K. Kwong, Opt. Lett. **10**, 454 (1985).
[7] P. Yeh, J. Opt. Soc. Am. B **2**, 1924 (1985).
[8] L.A. Lugiato, G.-L. Oppo, J.R. Tredicce, L.M. Narducci, and M.A. Pernigo, J. Opt. Soc. Am. B **7**, 1019 (1990).
[9] L.A. Lugiato, F. Prati, L.M. Narducci, P. Ru, J.R. Tredicce, and D.K. Bandy, Phys. Rev. A **37**, 3847 (1988).
[10] N.V. Kukhtarev, V.B. Markov, S.G. Odulov, M.S. Soskin, and V.L. Vinetskii, Ferroelect. **22**, 949 (1979).
[11] A. Yariv, *Quantum Electronics*, 3rd ed. (Wiley, New York, 1989).
[12] T.J. Hall, R. Jaura, L.M. Connors, and P.D. Foote, Prog. Quantum Electron. **10**, 77 (1985).
[13] P. Günter, Phys. Rep. **93**, 199 (1982).
[14] G. D'Alessandro and G.-L. Oppo, Opt. Commun. **88**, 130 (1992).
[15] G.L. Oppo, G. D'Alessandro, and W.J. Firth, Phys. Rev. A **44**, 4712 (1991).
[16] M. Brambille, M. Cattaneo, L.A. Lugiato, and F. Prati, *Proceedings of the Ecoosa '90 Conference*, edited by M. Bertolotti and E.R. Pike (IOP, Bristol, 1990).
[17] M. Brambilla, F. Battipede, L.A. Lugiato, V. Penna, F. Prati, C. Tamm, and C.O. Weiss, Phys. Rev. A **43**, 5090 (1991).
[18] L. Gil, K. Emilsson, and G.-L. Oppo, Phys. Rev. A **45**, R567 (1992).
[19] G.L. Oppo, L. Gil, G. D'Alessandro, and W.J. Firth, *Proceedings of the Ecoosa '90 Conference*, edited by M. Bertolotti and E.R. Pike (IOP, Bristol, 1990).

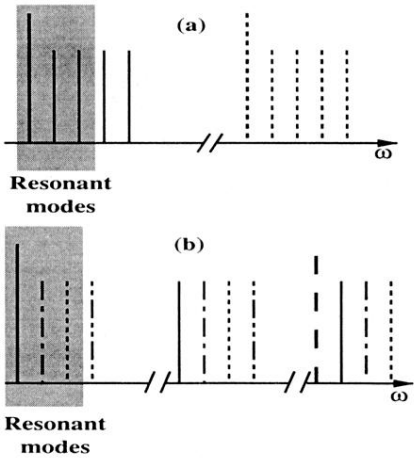

FIG. 2. Mode spectrum of a laser cavity. In (a) (nearly plane mirror cavity) the transverse-mode spacing is much smaller than the free spectral range and the transverse modes (short lines) are near their corresponding longitudinal mode (long lines). In (b) (nearly confocal cavity) the transverse modes belong to different longitudinal modes. The shaded areas indicate the modes that are relevant to the dynamics.

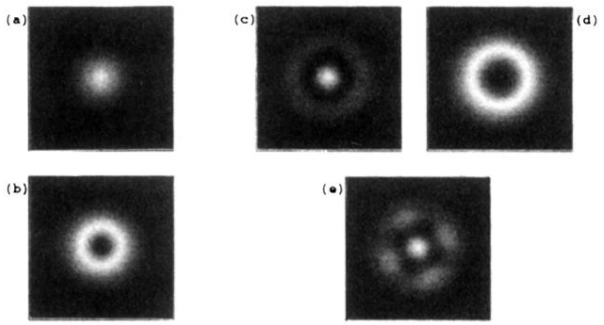

FIG. 4. Transverse-mode images: in these simulations $\tilde{a}$ is sufficiently large so that the pump is in resonance with only one family of transverse modes at a time. Gray scale, images of the intensity of the resonator field; white codes, high intensity; black, low intensity. $B = 1.4$, $\tilde{a} = 1.0$, $w = 5.0$. (a) $\Delta_{PR} = 0.0$, (b) $\Delta_{PR} = 1.0$, (c)–(e) $\Delta_{PR} = 2.0$.

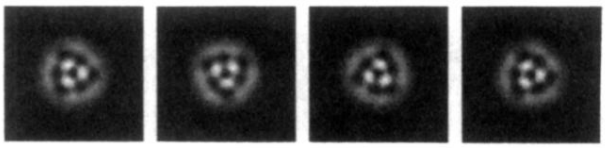

FIG. 5. Limit cycle of the resonator field. Gray scale, images of the intensity of the resonator field; white codes, high intensity; black, low intensity. The time interval between two successive images is 20. Time increases form left to right. $B = 1.1$, $\tilde{a} = 0.1$, $w = 5.0$, $\Delta_{PR} = 0.2$.

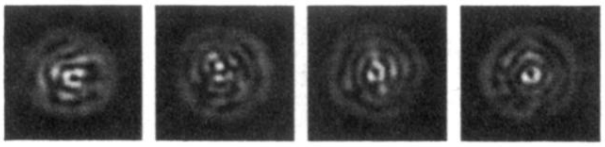

FIG. 6. Chaotic evolution of the resonator field. Gray scale images of the intensity of the resonator field, white codes high intensity, black low intensity. The time interval between successive images is 5. Time increases from left to right. $B = 1.8$, $\tilde{a} = 0.15$, $w = 5.0$, $\Delta_{PR} = 0.6$.